Journal of Pediatric Surgery (2007) **42**, 1561–1565

ELSEVIER

Journal of Pediatric Surgery

www.elsevier.com/locate/jpedsurg

Scanning electron microscopy of fetal murine myelomeningocele reveals growth and development of the spinal cord in early gestation and neural tissue destruction around birth

Dorothea Stiefel[a,b], **Martin Meuli**[b,*]

[a]*Neural Development Unit, Institute of Child Health, University College London, London, WC1N 1EH United Kingdom*
[b]*Department of Surgery, University Children's Hospital Zurich, Steinwiesstr. 75, 8032 Zurich, Switzerland*

Index words:
Myelomeningocele;
Spina bifida;
Neural tube defect;
Fetal surgery

Abstract

Background: Previous studies demonstrated that the spinal cord within a fetal myelomeningocele (MMC) lesion suffers progressive destruction during gestation. This study aims at elucidating this pathophysiologic feature on a cellular and ultrastructural level in a model of genetically determined MMC.

Methods: *Curly tail/loop tail* mouse fetuses at various gestational stages and neonates were analyzed electron-microscopically to document time-point and nature of neural tissue development and pathologic alterations within the MMC.

Results: At embryonic day (E) 8.5 and E9.5, round cells displaying multiple microvilli covered the entire region of interest, and some specimens showed initial stages of neurulation. At E10.5, neurulation was terminated in normal animals, whereas the neural placode remained unfolded in MMC fetuses and became distinguishable from adjacent epidermal layers. At E15.5, an apparently normal differentiation was found. Until this time-point, there was no tissue damage or inflammation. Thereafter, increasingly severe tissue alterations were identified with ongoing gestation leading to almost complete loss of neural tissue at birth.

Conclusion: We show here in fetal mice with MMC that, apart from absent neurulation, growth and development of the otherwise perfectly intact exposed spinal cord appear normal in early gestation, whereas later, the unprotected neural tissue is progressively destroyed.

Myelomeningocele (MMC), also known as spina bifida aperta (SB), is one of the most handicapping nonlethal congenital malformations in humans, leading to lifelong disabilities including paraparesis, hydrocephalus, structural brain anomalies, neuropathic bowel and bladder, sexual dysfunction, skeletal deformities, endocrine disorders, and impaired mental development [1,2]. The prevalence lies at around 1 per 1000 live births, with considerable geographic variation [1,3]. The etiology of this devastating neural tube defect is not fully understood; however, genetic as well as environmental factors are definitely involved [4]. Until some years ago, the severe neurologic deficit associated with MMC was believed to be a direct consequence of the primary

* Corresponding author.
E-mail address: martin.meuli@kispi.unizh.ch (M. Meuli).

0022-3468/$ – see front matter © 2007 Elsevier Inc. All rights reserved.
doi:10.1016/j.jpedsurg.2007.04.019

disorder, namely, failure of neurulation of the spinal cord. Recent evaluations of human fetuses with MMC as well as a considerable body of experimental data from various animal models have shown that secondary, that is, in utero acquired, progressive destruction of the pathologically exposed part of the spinal cord is an important, if not the main, factor causing the neurologic disaster commonly found at birth [5-10]. In a previously conducted study, we could histologically document in a mouse model with naturally occurring SB that the openly exposed and hence unprotected spinal cord within the lesion was progressively destroyed with ongoing gestation. In more detail, various histologic techniques applied in these experiments have shown that the first visible tissue alterations start at embryonic day (E) 15.5 (term, E19.5), whereas at term (=E19.5), the neural tissue was almost completely lost [11]. The present study was designed to elucidate the prenatal natural neural tissue alterations on a cellular and ultrastructural level using electron microscopy to detect even the most subtle and early-occurring changes.

Table 1 Essential morphological findings in control and MMC animals at various points of gestation

Gestational age	Control animals	MMC animals
E8.5	Intact round cells with microvilli	Intact round cells with abundant microvilli
E9.5	Idem	Idem
E10.5	Neural tube closure completed	Persistent neural placode, epidermis and neuroepithelium discernable, no microvilli
E14.5		Abundant proliferating cells, surface intact, no inflammatory response
E15.5		Irregular surface, signs of tissue erosion/abrasion within lateral parts of placode, significant loss of neural tissue
E16.5		Idem
E17.5		Massive loss of neural tissue
E18.5		Neural tissue almost completely lost
P1		Neural tissue completely lost

1. Materials and methods

1.1. Mouse strains and collection of specimens

Inbred *curly tail/loop tail* mice were maintained on a 12-hour light-dark cycle. Overnight mating between heterozygous *loop tail/curly tail* males (*Lp/+;ct/+*) and homozygous *curly tail* females *(+/+;ct/ct*) were checked for vaginal plugs the following morning and designated as E0.5 in case of positive copulation. Because murine physiologic neurulation starts at E8.5, experimental litters were collected daily from E8.5 to E18.5 and on the first postnatal day (P) 1 (E19.5 = P1). Unaffected littermates were used as control animals (CTs).

Embryos were collected after pregnant females were culled by cervical dislocation, whereas neonates were collected after females had littered. Embryos were dissected out into Dulbecco's modified Eagle's medium (Gibco BRL Life Technologies, LTD, Paislea, United Kingdom) containing 10% fetal calf serum. The extraembryonic membranes were removed and the animals rinsed in phosphate-buffered saline. Specimens older than E15.5 were killed on a frozen metal plate before fixation, whereas younger embryos were placed directly into fixatives. Thereafter, all animals were processed for scanning electron microscopy.

1.2. Scanning electron microscopy

Specimens were collected as described (n = 57; E8.5, 4; E9.5, 6; E10.5, 4 SB; E11.5, 9 SB + 2CT; E12.5, 9 SB; E13.5, 8 SB + 1 CT; E14.5, 4 SB; E15.5, 2; E16.5, 2 SB; E17.5, 2 SB; E18.5, 2 SB; P1, 2 SB). To facilitate handling of the delicate tissue after the process of critical point drying, a fine cactus spine was run through the animal. Specimens were then stuck on a layer of 10% agarose and placed in the fixative containing 3% glutaraldehyde so that the MMC lesion was freely surrounded by the fixative. Specimens were fixed for at least 48 hours. The older SB animals (E14.5-P1) were then cut at informative planes with a fine scalpel blade; the younger specimens were kept intact. After several washes with dH2O, the specimens were postfixed in 1% osmiumtetroxide for 30 minutes, washed again, and serially dehydrated. Covered with 100% ethanol, the animals were transferred into the chamber of the critical point dryer and dried from liquid carbon dioxide. Mounted on aluminum stubs with double-sided adhesive tape, they were finally sputter-coated with gold for 3 minutes under 20 mA argon vacuum. Specimens were examined using a JEOL JSM35 scanning electron microscope at 25kV (JEOL Scanning electron microscope 35, Hertfordshire, UK).

1.3. Photographic documentation

Photographic documentation for scanning electron microscopy was obtained with black and white films.

2. Results

Mating between heterozygous *Lp/ct* males and homozygous *ct/ct* females generated litters with 3 different phenotypes: in 34%, animals with a classical MMC of varying size located in the lumbosacral region; in 25.5%, pups without SB, but with a curly, kinky, or looped tail; and

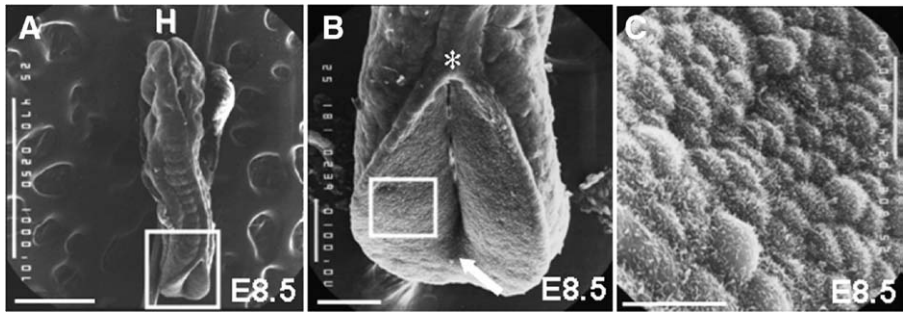

Fig. 1 Findings at E8.5. A, Top view of dorsal aspect of an embryo before completed neurulation. Whereas neural tube closure has already occurred in the midportion, the anterior (rostral) neuropore (top) as well as the posterior (caudal) neuropore (bottom) are still open. At this time, it cannot yet be determined whether the animal has SB. H indicates head. Scale bar, 500 μ. B, Top view of the posterior neuropore area (box in A). Rostrally, the neural folds have fused to form the neural tube (asterisk), whereas more caudally, the neural placode appears wing-shaped, with a central groove that will become the central canal in normal animals or remain open in SB animals (arrow). Scale bar, 100 μ. C, Close-up view of superficial cell layer of the placode (box in B). The round cells are densely packed and appear intact and healthy. The visible cell surface consists of microvilli. Scale bar, 10 μ.

in 39.5%, entirely normal animals. The latter 2 groups served as CTs. A total of 57 animals were collected from stages E8.5 to P1.

The main findings are summarized in Table 1.

At E8.5 and E9.5, the specimens showed signs of ongoing neural tube closure (various stages of neural placode folding). On scanning electron microscopy, all E8.5 and E9.5 specimens demonstrated uniform round cells on the entire surface, not allowing distinction between tissues of epidermal or neural origin, respectively. All cells displayed abundant microvilli, suggesting a particularly active metabolism at this time (Fig. 1).

At E10.5, neurulation was completed in normal animals, whereas a clearly discernable MMC became apparent in the affected animals. Also, at E10.5, a clear-cut distinction between the neural tissue (cobblestonelike appearance) of the placode and the adjacent epidermal (squamous and flat cells) layer was possible. Both cell types were devoid of microvilli. No signs of inflammation or tissue damage were detectable (Fig. 2).

At E14.5, the neural tissue was still perfectly intact, and differentiation into alar and basilar plate was completed with many proliferating cells. There were no signs of tissue damage or inflammatory response. At E15.5 and E16.5, the placode surface assumed an inhomogeneous and irregular aspect because of flattening and tissue erosion/abrasion, particularly in the most lateral portions of the placode, which are the most exposed parts of the neuroepithelium.

At E17.5 and E18.5, there was progressive disruption and loss of neural tissue within all parts of the neural placode (Fig. 3). At P1, we found a near-total or, in some specimens, an even complete loss of all formerly present neural tissue (Fig. 4).

3. Discussion

This electron-microscopic study shows that mouse fetuses with spontaneous MMC demonstrate an intact nonneurulated spinal cord with apparently normal differentiation in early gestation, whereas later gestational stages are characterized by progressive secondary neural tissue damage that starts with subtle cellular changes and progresses to complete loss of neural tissue around birth. In more detail, between E10.5

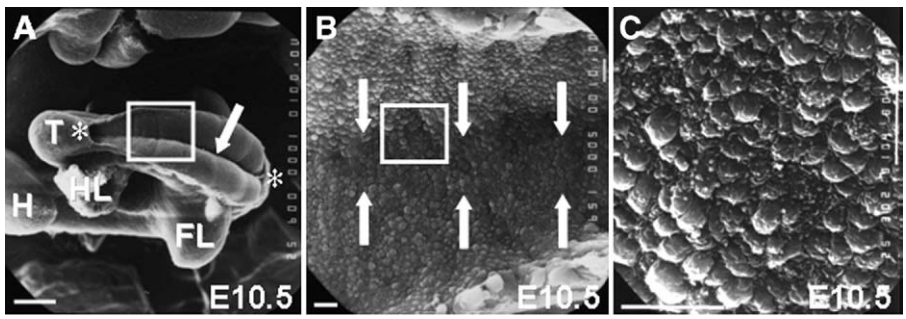

Fig. 2 Findings at E10.5. A, Top view of dorsal aspect of an SB animal. The nonneurulated, but intact, placode is clearly discernable between the 2 asterisks. The central canal area forms a midline groove (arrow). T indicates tail; HL, hindlimb buds; FL, forelimb buds; H, head. Scale bar, 200 μ. B, Higher-magnification view (box in A) of central area of the placode including midline groove (between arrows). The round cells are still densely packed and uniform, and there is no evidence of compromised tissue integrity. Scale bar, 10 μ. C, Close-up view of midline groove area (box in B). Cells are round, intact, and devoid of microvilli. Scale bar, 10 μ.

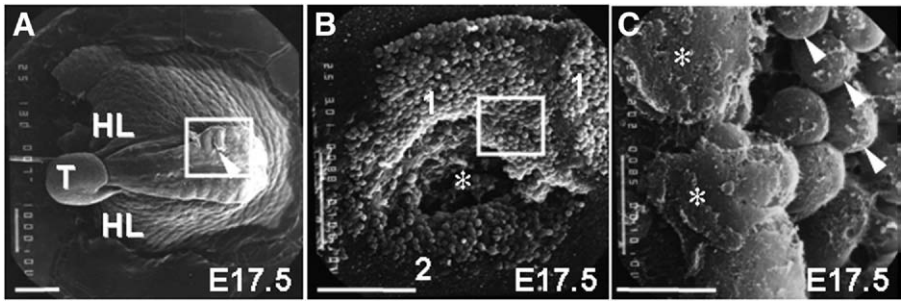

Fig. 3 Findings at E17.5. A, Overview of lumbar-sacral area with notable irregularities within the neural placode. The filled arrowheads point at tissue disruptions. T indicates tail; HL, hindlimb. Scale bar, 1 mm. B, Detail view of an area (box in A) with a holelike formation within the placode (asterisk). There are areas still densely populated by cells (1), whereas other parts of the placode show less (2) cells. Scale bar, 100 μ. C, Close-up view of single neural cells of various sizes and shapes (box in B). The round cells (filled arrowheads) still appear normal, whereas the cells in the foreground (asterisks) appear flattened and show marked surface irregularities as if crushed by external mechanical forces. Scale bar, 10 μ.

and E14.5, the persistent neural placode is characterized by an apparently normal differentiation into alar and basilar plate; by the presence of abundant proliferating and metabolically active cells consistent with growth and development; and by a perfectly intact neural tissue surface as well as no evidence for an inflammatory response, reflecting absence of morphologically detectable neural damage. Between gestational stages E15.5 and P1, however, we observed increasingly severe changes, from altered cell shape to cell necrosis, surface irregularities, tissue erosion, tissue disruption, hemorrhage, inflammatory cell infiltration, and, finally, plain and definitive loss of spinal cord tissue within the lesion. Because these data are gathered without any external manipulation in an animal model with naturally occurring, classical SB, it is correct to conclude that they describe the prenatal natural pathomorphology of MMC.

There is only 1 similar study available for comparison, where McLone et al [12] investigated fetal delayed splotch mice, a mutant mouse strain similarly characterized by genetically determined SB. The authors also found a normal development of the nonneurulated placode in early gestation. However, although they described cell death, loss of superficial ependymal covering, and a significantly reduced tissue volume near term, they did not report massive tissue destruction to the same extent as we did. The reason for this possibly milder manifestation of secondary neural tissue damage is difficult to explain, particularly because the 2 mouse models resemble each other very closely [12].

Importantly, studies on therapeutically aborted pregnancies and stillborn human fetuses with MMC have demonstrated that the exposed part of the spinal cord within the MMC lesion has failed to neurulate, but otherwise appears to develop the normal anatomical hallmarks in early gestation, and then suffers progressive tissue destruction with ongoing gestation [5,7,9,10].

Finally, there is a substantial body of evidence stemming from numerous fetal animal models with surgically induced MMC proving that normal spinal cord tissue exposed for a significant period to the amniotic cavity is progressively destroyed [8,10,13-15].

Taken together, there are now ample confirmative data from the present and the quoted studies leading to the conclusion that secondary, in utero acquired, progressive destruction of the pathologically exposed spinal cord tissue is a characteristic, late-gestational phenomenon in the prenatal natural history of MMC. Clearly, the identification of late-

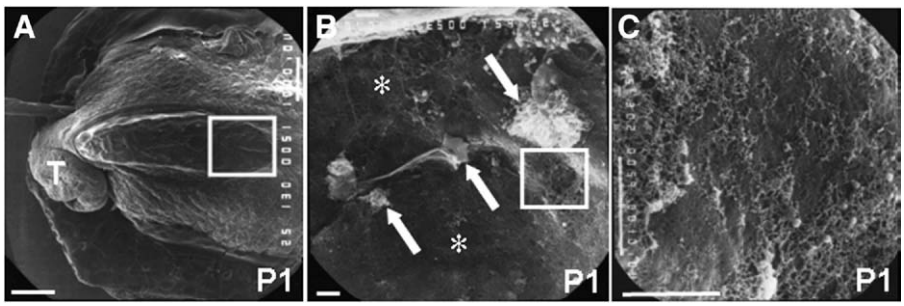

Fig. 4 Findings at P1. A, Top view of neonatal SB animal. The former neural placode has disappeared within the entire lesion. Eventual tiny neural remnants cannot be identified at this magnification. T indicates tail. Scale bar, 1 mm. B, Detail view of area (box in A) where neural tissue is completely missing. Arrows point at unidentifiable detritus, possibly of neural origin. The visible surface consists of cartilaginous tissue lining the ventral aspect of the open spinal canal (asterisk). Scale bar, 10 μ. C, Close-up view of the box area in B. "Sandy" detritus is laying dispersed on cartilaginous ground. Scale bar, 10 μ.

gestational secondary neural tissue damage corroborates the concept of timely fetal surgery for human fetuses with MMC aiming at averting the serious neurologic deficit by early protective coverage of the spinal cord tissue [16,17].

In conclusion, this ultrastructural study has produced further evidence that the nonneurulated spinal cord is intact and develops normally in early gestation, whereas the exposed neural tissue is subject to a massive destruction process in later gestation, leading to near-total loss of all formerly exposed neural tissue around birth. These findings are in line with the current rationale for prenatal intervention in human fetuses affected by this devastating congenital malformation.

Acknowledgment

We would like to thank Professor AJ Copp at the Institute of Child Health, London, United Kingdom, for his support and critical insights, and K Verner, laboratory technician at the National Hospital of Neurology and Neurosurgery, London, United Kingdom, for her technical support during the study.

References

[1] Bouchard S, Davey MG, Adzick NS, et al. Correction of hindbrain herniation and anatomy of the vermis after in utero repair of myelomeningocele in sheep. J Pediatr Surg 2003;38:451-8.

[2] Dias MS, McLone DG. Hydrocephalus in the child with dysraphism. Neurosurg Clin N Am 1993;4:715-26.

[3] Babcook CJ, Goldstein RB, Filly RA, et al. Prevalence of ventriculomegaly in association with myelomeningocele: correlation with gestational age and severity of posterior fossa deformity. Radiology 1994;190:703-7.

[4] Manning SM, Jennings R, Madsen JR. Pathophysiology, prevention, and potential treatment of neural tube defects. Ment Retard Dev Disabil Res Rev 2000;6:6-14.

[5] Emery JL, Lendon RG. Clinical implications of cord lesions in neurospinal dysraphism. Dev Med Child Neurol 1972;14(Suppl 27): 45-51.

[6] Korenromp MJ, Van Gool JD, Bruinse HW. Early fetal leg movements in myelomeningocele. Lancet 1986;1:917-8.

[7] Osaka K, Tanimura T, Matsumoto S, et al. Myelomeningocele before birth. J Neurosurg 1978;49:711-24.

[8] Heffez DS, Aryanpur J, Freeman JM, et al. The paralysis associated with myelomeningocele: clinical and experimental data implicating a preventable spinal cord injury. Neurosurgery 1990;26: 987-92.

[9] Hutchins GM, Meuli M, Blakemore KJ, et al. Acquired spinal cord injury in human fetuses with myelomeningocele. Pediatr Pathol Lab Med 1996;16:701-12.

[10] Meuli M, Meuli-Simmen C, Adzick NS, et al. The spinal cord lesion in human fetuses with myelomeningocele: implications for fetal surgery. J Pediatr Surg 1997;32:448-52.

[11] Stiefel D, Copp AJ, Meuli M. Fetal Spina bifida in a mouse model: loss of neural function in utero. J Neurosurg 2007;(3 Suppl Pediatrics): 213-21.

[12] McLone DG, Dias MS, Knepper PA, et al. Pathologic changes in exposed neural tissue of fetal delayed splotch (Spd) mice. Childs Nerv Syst 1997;13:1-7.

[13] Michejda M. Intrauterine treatment of spina bifida: primate model. Z Kinderchir 1984;39:259-61.

[14] Drewek MJ, Bruner JP, Tulipan N. Quantitative analysis of the toxicity of human amniotic fluid to cultured rat spinal cord. Pediatr Neurosurg 1997;27:190-3.

[15] Olguner M, Akgur FM, Ozer E, et al. Amniotic fluid exchange for the prevention of neural tissue damage in myelomeningocele: an alternative minimally invasive method to open in utero surgery. Pediatr Neurosurg 2000;33(5):252-6.

[16] Hirose S, Meuli-Simmen C, Meuli M. Fetal surgery for myelomeningocele: panacea or peril? World J Surg 2003;27(1):87-94.

[17] Walsh DS, Adzick NS. Foetal surgery for spina bifida. Semin Neonatol 2003;8:197-205.